Increase of superfluid density with growth of quasiparticle density of states probed by intrinsic tunneling spectroscopy in Bi$_{1.9}$Pb$_{0.1}$Sr$_2$CaCu$_2$O$_{8+\delta}$

Hitoshi Kambara,[*] Itsuhiro Kakeya,[†] and Minoru Suzuki

Department of Electronic Science and Engineering, Kyoto University, Kyoto, Japan

Interlayer tunneling spectra, the Josephson critical current density J_c, and the normal tunneling resistance have been measured simultaneously for intrinsic Josephson junctions of Bi$_{1.9}$Pb$_{0.1}$Sr$_2$CaCu$_2$O$_{8+\delta}$ (BiPb2212) in the underdoped region using a small mesa structure ($S = 1 \times 1$ μm^2) and a short-pulse technique. J_c was significantly enhanced when Bi was partially replaced with Pb. By comparing J_c with the value estimated by the Ambegaokar-Baratoff formula, it was found that superfluid density doubles in the Pb-containing sample. In addition, Pb raises the superconducting coherence peak without changing the value of the superconducting gap Δ. Based on a model that accounts for the inhomogeneity of Δ in $\boldsymbol{k}$ space, we argue that the superfluid density increases because Pb substitution increases the homogeneity of $\Delta(\boldsymbol{k})$.

I. INTRODUCTION

The crystal structures of cuprate superconductors comprise layers of superconducting CuO$_2$ atomic sheets interspersed with layers of insulating sheets. The interfaces between the layers are termed intrinsic Josephson junctions (IJJs).[1] Intrinsic tunneling spectroscopy (ITS) is a technique by which information on the quasiparticle density of states (DOS) in the CuO$_2$ layers can be extracted from the c-axis current-voltage characteristics.[2–4] Since an IJJ inside the crystal is protected by other IJJs, ITS probing enables us to access bulk quasiparticle DOS that are protected from surface deterioration. This feature contrasts sharply with surface sensitive spectroscopic probes such as angle-resolved photoemission spectroscopy (ARPES)[5–7] and scanning tunneling spectroscopy (STS).[8–10] These probes have revealed that the pseudogap[11] survives even above the superconducting transition temperature T_c. Thus the electronic phase diagram of cuprates can be fully elucidated. More recently, the energy resolution of these spectroscopic probes has been greatly improved, allowing segregations of the superconducting gaps and the pseudogaps in the momentum space ($\boldsymbol{k}$ space) to be recognized, which is referred to as Fermi arc.[12,13]

More relevant to this work, ITS allows simultaneous measurements of the Josephson critical current density J_c (given by the superfluid tunneling component) and the quasiparticle DOS. In a Josephson junction composed of conventional superconductors, J_c at a sufficiently low temperature is proportional to the superconducting gap Δ by the Ambegaokar-Baratoff formula[14]

$$J_c^{\mathrm{AB}} \approx \frac{\pi \Delta}{2 e R_{\mathrm{N}} S}, \tag{1}$$

where R_{N} is the normal tunneling resistance, S is the area of the Josephson junction, and e is the elementary charge. From this relationship, we infer that the higher the T_c is, the higher the J_c is in the Josephson junction. Clearly, this relationship does not hold for c-axis Josephson tunneling in cuprates, because their T_c's vary quadratically with increasing carrier concentrations while their J_c's increase exponentially.[15] Furthermore, previous ITS measurements for Bi$_2$Sr$_2$CaCu$_2$O$_{8+\delta}$ (Bi2212)[15] have revealed that J_c is smaller than J_c^{AB} by two

orders of magnitude in the underdoped region, and the ratio J_c/J_c^{AB} increases as the carrier concentration increases. With increasing carrier concentration, the Fermi arc extends in both (π, 0) and (0, π) directions to form a closed Fermi surface.[6,13] Given that J_c suppression and shrinking Fermi arc depend similarly on the doping dependence, we infer that J_c/J_c^{AB} is a macroscopic measure of the incompleteness of the Fermi surface.[15] Investigations on IJJ materials with varying J_c would provide intriguing tests of this idea. Substituting Bi with Pb is known to drastically increase the critical current density of Bi cuprates, Bi$_2$Sr$_2$Ca$_{n-1}$Cu$_n$O$_{2n+4+\delta}$ ($n = 1, 2, 3$).[16] This enhancement of J_c is attributed to structural changes in the BiO block layers rather than increased carrier concentration. Essentially, the Pb substitution orders the block layer and lowers the barrier height.[17–19] We have previously found that Pb substitution increases J_c beyond that expected from the change of resistivity.[19]

In this paper, we discuss the effect of the Pb substitution on J_c, the quasiparticle DOS in the $\boldsymbol{k}$ space, and the superconducting gap structure. We measured J_c, Δ, and R_{N} in Pb-substituted Bi2212 (BiPb2212) by ITS. We then estimated J_c^{AB} from Δ and R_{N}, and determined J_c/J_c^{AB}. We found that the anomalously reduced J_c was recovered by the Pb substitution. Moreover, by comparing the tunneling spectra with those of Bi2212 and calculations, we conclude that Pb substitution enlarges the Fermi arc and increases the J_c.

II. EXPERIMENTS

Single crystals (nominal composition of Bi$_{1.8}$Pb$_{0.2}$Sr$_2$CaCu$_2$O$_{8+\delta}$) used in the present work had been grown previously by the self-flux method.[20] Electron dispersive spectroscopy (EDS) reveals a homogeneous distribution of Pb within the crystal, and a composition of Bi$_{1.9}$Pb$_{0.1}$Sr$_2$CaCu$_2$O$_{8+\delta}$. To ensure identical Pb concentrations among the samples, crystals with flat surfaces (*ab* plane) were collected from aggregates grown in the same crucible. To obtain Hall-bar and mesa structures, crystals were fabricated under vacuum conditions. Basic properties of the samples are listed in Tables I and II.

TABLE I. Physical properties and sample dimensions of Hall-bar samples H-1-3.

Sample	H-1	H-2	H-3
T_c (K)	84.2	82.9	88
R_H (300 K) (10^{-3} cm^3 C^{-1})	2.21	2.12	1.72
p	0.124–0.140	0.126–0.142	0.138–0.150
Thickness: d (nm)	62.1	123.3	346.1

Differences between samples are caused by changing oxygen concentrations throughout the processes in vacuum.

Samples H-1, H-2, and H-3 were used for *ab*-plane transport measurements. The Hall-bar patterns were formed by photolithography with either wet or dry etching in thin (<500 nm) crystals cleaved from the single crystals. A prepared sample with silver electrodes is shown in Fig. 1(a). Resistances and Hall voltages are measured simultaneously with the ac standard bridge of the Physical Properties Measurement System (Quantum Design Inc.). The scanning external magnetic field was set perpendicular to the Hall-bar plane and was varied between $\mu_0 H = \pm 1$ T.

Samples M-1, M-2, and M-3 were used for the *c*-axis transport measurements. Mesa structures of a few unit cells thickness (surface area 1×1 μm^2) were fabricated by cleave-in-vacuum method[21] and electron-beam lithography.[20] Our method[20] allows the thickness of the mesa to be controlled to half-unit-cell precision (1.5 nm). The mesas shown in Fig. 1(b) were measured by the three probe technique, assuming negligible contact resistance between the mesa and the upper electrode. The *c*-axis resistance was measured by standard dc methods, and the current-voltage (*I-V*) characteristics were collected under a constant-amplitude biasing triangular ac voltage. ITS measurements were performed with the short pulse (~1 μs) bias method[2] to maximally suppress self-heating in high bias regions. Details of sample preparation and measurement are described elsewhere.[19,20]

III. RESULTS AND DISCUSSION

A. *ab*-plane transport measurements

Figure 2 shows how the *ab*-plane resistivity $\rho_{ab}(T)$ and the Hall coefficient $R_H(T)$ vary with temperature. A typical Hall-bar sample (H-3) of thickness $d = 346$ nm was used. We define T_c as the midpoint of the resistance drop starting around 100 K. The obtained T_c values are consistent with those

of bulk BiPbi2212 crystals obtained from the same crucible. $R_H(T)$ exhibits a broad peak around 130 K associated with T-linear behavior at a higher temperature region and a rapid decrease in the lower temperature region. These $R_H(T)$ trends are commonly observed in cuprate superconductors.[22] Among the samples, sample H-3 with the highest T_c shows the smallest R_H(300 K) [see Table I], which tells that all of the samples are underdoped.

B. Estimation of hole doping

The extent of doping p in the mesa must be determined in this study, since we aim to compare the doping evolution of the superconducting gap and Josephson critical current between BiPb2212 and Bi2212. In BiPb2212, p cannot be directly determined by cation substitution because the excess oxygen located between the BiO planes introduces hole carriers into the CuO$_2$ layers.[23,24] According to Ando *et al.*[25] and Konstantinović *et al.*,[26] p can be determined by comparing the hole number per Cu atom n_H^{Cu} at 300 K in various cuprates with that in La$_{2-x}$Sr$_x$CuO$_4$ (LSCO), for which p is equal to x. Applying this approach, we obtained p as 0.124–0.150 from the measured values of $n_H^{Cu} = 0.31$–0.41. From these results, we obtain the following empirical formula[27] for determining $T_c(p)$ of the BiPb2212:

$$\frac{T_c}{T_c^{\max}} = 1 - 82.6(p - 0.16)^2, \qquad (2)$$

where $T_c^{\max}$ is 89.7 ± 0.5 K. The doping p's of the mesas listed in Table II are estimated by Eq. (2) from the measured T_c vice versa. For all of the samples used in this study, p is below 0.16, inconsistent with an interpretation that substituting Bi^{3+} with Pb^{2+} in Bi2212 increases hole carriers in the CuO$_2$ layers and makes the crystals overdoped. We posit instead that the Pb substitution decreases the volume of excess oxygen near the substitution site. In fact, the excess oxygen trapped between the BiO planes modifies the crystal structure;[28,29] thus the

TABLE II. Physical properties and sample dimensions of mesa samples M-1-3.

Sample	M-1	M-2	M-3
T_c (K)	63.5	77	86.5
Δ(10 K) (meV)	36	37.3	32.3
J_c(10 K) (kA/cm^2)	2.4	4	10
J_c^{AB}(10 K) (kA/cm^2)	43.6	48.2	51.1
R_N(10 K) (Ω)	129.5	121.5	99.2
ρ_c(300 K) (Ω cm)	11.3	10.3	7.88
p	0.098–0.103	0.115–0.123	0.132–0.148
Number of IJJs: N	5	4	4
Area: S (μm^2)	1×1	1×1	1×1
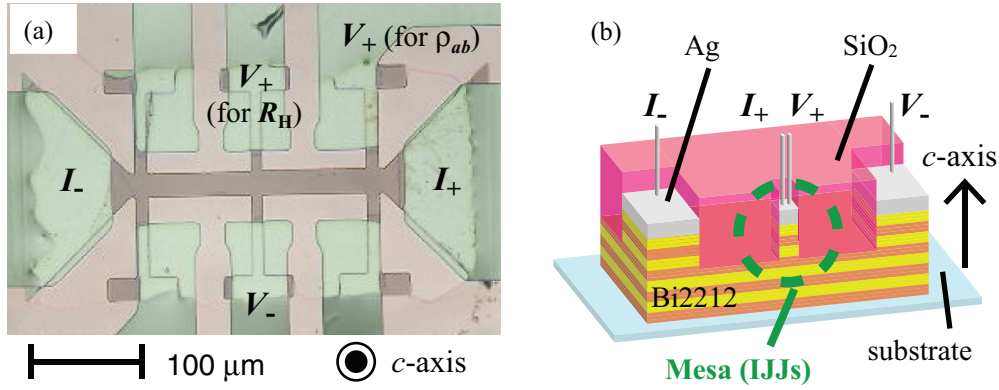
FIG. 1. (Color online) Photograph of a Hall-bar sample (a) and a schematic illustration of a mesa structure (b).

presence of Pb reduces the significance of the modulation of the ab plane.[16,30]

C. ITS measurements

Figure 3(a) shows the relationship between temperature and c-axis resistivity ρ_c of the mesas. T_c is defined as the midpoint of the resistive transition. As temperature decreases up to T_c, ρ_c increases to several times larger than that at room temperature, and suddenly drops thereafter. This remarkable change in ρ_c is characteristic of underdoped Bi2212.[15,31] In addition, the magnitude of ρ_c and the extent of its rise increase with decreasing T_c. These features further suggest that all of the mesas are underdoped. However, the ρ_c values are several times smaller than those of Bi2212, suggesting that the structural modifications in-

FIG. 2. Temperature dependence of the ab-plane resistivity ρ_{ab} (a) and the Hall coefficient R_H (b) for the sample H-3.

duced by the Pb substitution[18] lower the tunnel barrier of the IJJ.

Figures 3(b)–3(d) exhibit the c-axis I-V characteristics for the respective mesas. The homogeneous critical current for all branches and equal voltage spacing between the branches demonstrate that the IJJs within the mesas possess identical properties. The number of junctions N included by each mesa is clearly indicated by the number of branches in the figures. Furthermore, because the first branch in each mesa is perpendicular to the voltage axis, the contact resistance of each mesa is sufficiently low. Therefore, we can extract quasiparticle tunneling properties for a single IJJ by dividing the observed voltage by the number of junctions. The Josephson critical current densities J_c ranged from 2 to 10 kA/cm^2, much larger than those of Bi2212, which ranged from 0.2 to 1 kA/cm^2 at $p = 0.10$–0.14.[15]

Figure 4 displays the results of ITS measurements for the same mesas. The I-V curves are linear in the high voltage region (>120 mV), implying that the self-heating induced by the bias current is sufficiently suppressed. Thus we can determine the normal tunneling resistance R_N from the slope of the I-V characteristics in the linear region. When self-heating is not negligible, sublinear behavior occurs in the high voltage region of the I-V curve.[32] The dI/dV magnitudes of the tunneling spectra display sharp peaks, characteristic of superconducting gaps below T_c. The superconducting gaps ($\Delta = 30$–40 meV at $T = 10$ K) are the same as those for underdoped Bi2212.[15] However, as shown later, the peak magnitudes exceed those of Bi2212 in the same doping region. We also observe another gap structure ($>2\Delta$) that dips and rises below T_c and survives at temperatures exceeding T_c. This can be interpreted as the pseudogap.[15]

D. Doping dependence of Josephson critical current density

As shown in Figs. 3(b)–3(d), since the Josephson critical current is homogenous within the stacked IJJs, J_c can measure bulk superconducting properties in addition to Δ. Here, the doping dependences of J_c and the superconducting gap structures of BiPb2212 and Bi2212 are compared. As already discussed, the Josephson critical current density J_c^{AB} in an s-wave superconductor at a low temperature is given by Eq. (1).[14] Since the J_c^{AB} differs between s wave and d wave by an order of unity,[33] Eq. (1) is applicable to our analysis. In
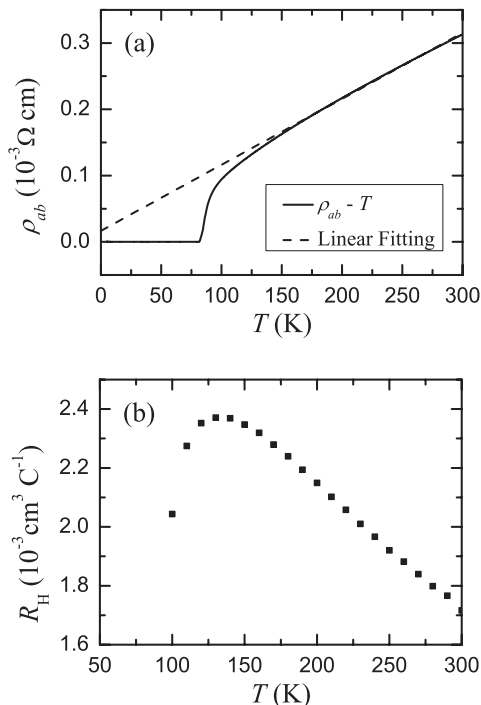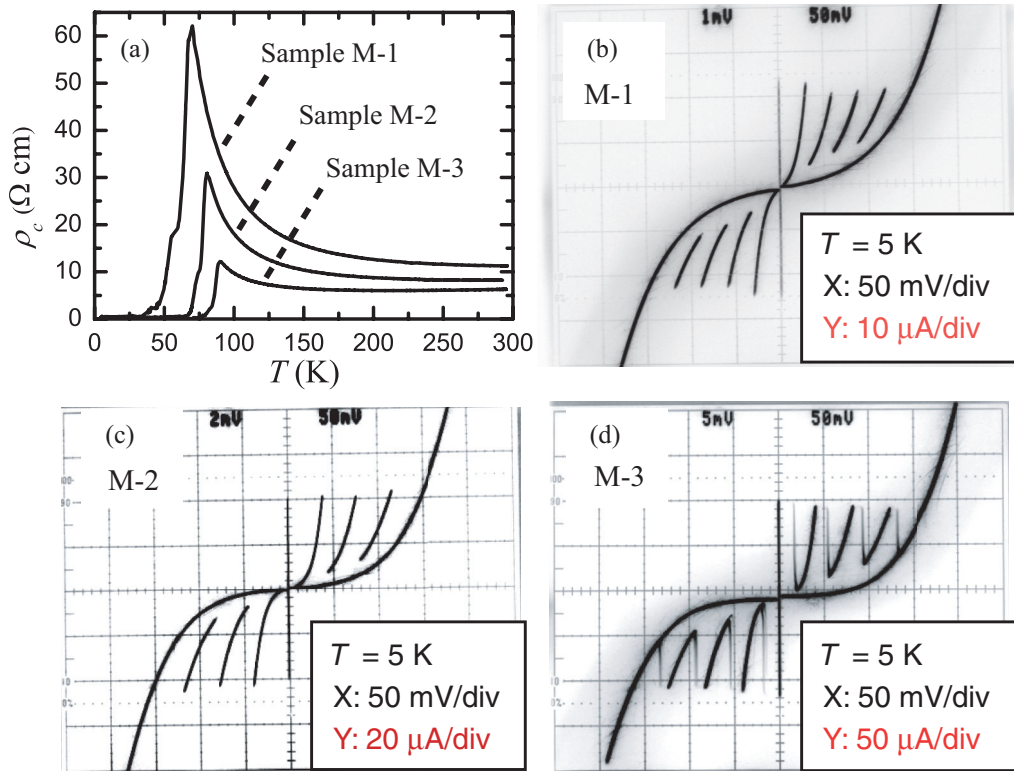
FIG. 3. (Color online) Temperature dependence of the c-axis resistivity ρ_c (a) and I-V characteristics obtained by an analog oscilloscope at 5 K (b)–(d) for the mesa samples.

the present study, J_c, R_N, and Δ are independently determined from Figs. 3(b)–3(d), 4(a)–4(c), and 4(d)–4(f), respectively. Figure 5 shows how J_c^{AB}, J_c, and the ratio J_c/J_c^{AB} vary with p in both Bi2212 and BiPb2212. Previous experiment has shown that J_c in underdoped Bi2212 is more than an order of magnitude smaller than J_c^{AB}.[15] It is also known that as p

decreases, J_c becomes more suppressed. For instance, J_c/J_c^{AB} decreases from 0.067 to 0.027 as p decreases from 0.14 to 0.10.[15] A similar result is obtained for BiPb2212, although the magnitudes of both J_c^{AB} and J_c are larger than those of Bi2212 due to the lowered R_N values (relative to Bi2212). However, the extent of the suppression is quantitatively smaller in the
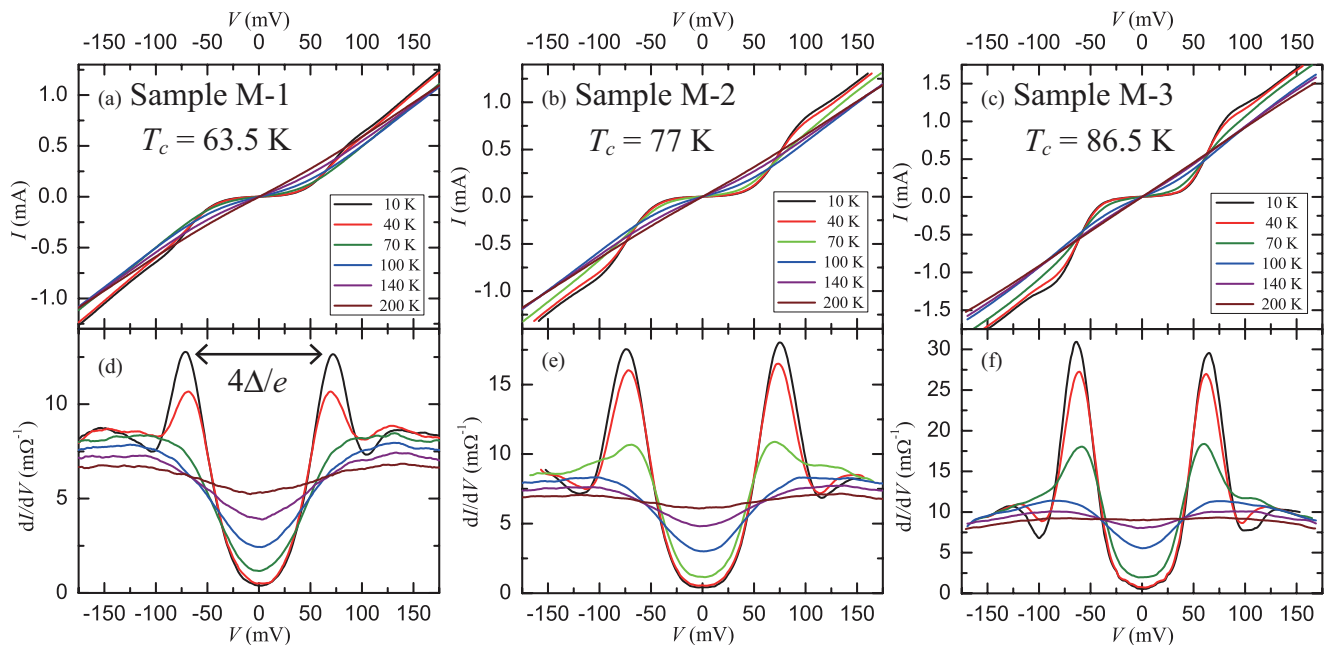
FIG. 4. (Color online) I-V curves measured by short-pulse ITS (a)–(c) and tunneling spectra (d)–(f) for the mesa samples. In this figure, the horizontal axis is normalized to the single junction voltage by dividing the observed voltage by the number of junctions.
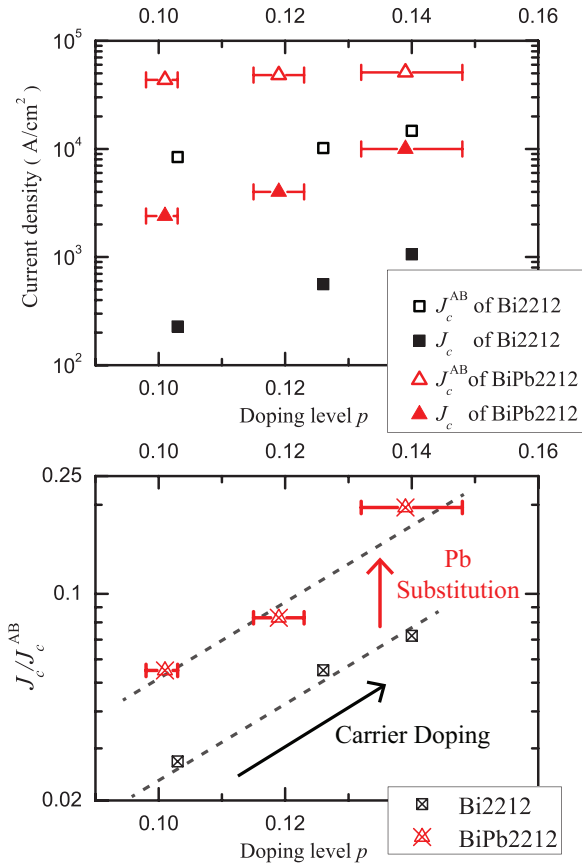
FIG. 5. (Color online) Plots for J_c, J_c^{AB}, and J_c/J_c^{AB} as a function of p for BiPb2212 (this work) and Bi2212 (Ref. 15).

FIG. 6. (Color online) Comparison between normalized tunneling spectra of a Bi2212 sample (black line; the sample C in Ref. 15) and a BiPb2212 sample (red-dotted line; the sample M-2 in this work) with close p. Each tunneling spectrum is normalized by dividing each spectrum by each value at $V = 150$ mV because the values at high voltage correspond to the density of states in the normal states.

present case than that for Bi2212. For example, around $p = 0.10$, J_c/J_c^{AB} is 0.027 and 0.055 for Bi2212 and BiPb2212, respectively. Since the change in J_c/J_c^{AB} is not explained by the reduced R_N, the Pb substitution must enhance the superfluid density by a factor of 2.

In our previous ITS studies on Bi2212, we posited that such anomalous suppressions of J_c result from inhomogeneous superconductivity.[34] The Josephson current flows only when both junction electrodes are in the superconducting (SC) state. When this is not the case, the junction is resistive and no Josephson current flows. If the SC state is inhomogeneous, the Josephson current will flow in some regions but not in others. When a sheet of the CuO_2 plane appears randomly fractionalized into SC and nonsuperconducting (NSC) regions, the J_c decreases according to the degree of fractionalization. This model is supported by microscopic spatial inhomogeneity of the Δ values on the surface ab planes of pristine Bi2212 crystals, revealed by STS experiments.[8] Similar inhomogeneity has been reported in the Δ of BiPb2212.[9] The standard deviation of the Δ distribution is very similar in BiPb2212 and Bi2212.[10] According to the real space inhomogeneity model, the extent of J_c suppression is mirrored in the spatial distribution of SC and NSC regions. However, our results showed that the suppression is significantly weakened in BiPb2212. Thus we argue that inhomogeneous superconductivity in real space cannot fully account for the increased J_c/J_c^{AB} in BiPb2212.

We suggest instead that the Pb substitution increases the length of the Fermi arc, which weakens the extent of J_c suppression. This suggestion is justified by a model that explains the anomalous suppression of J_c in underdoped Bi2212, in terms of $\boldsymbol{k}$-space inhomogeneity in the superconducting gap.[15] This $\boldsymbol{k}$-space inhomogeneity model predicts that superfluid density and J_c in a d-wave superconductor drastically decrease when the $\Delta(\boldsymbol{k})$ around the antinodal, $(\pi, 0)$ and $(0, \pi)$, directions in the $\boldsymbol{k}$ space disappears.[15] ARPES experiments have revealed that Δ grows in regions of $\boldsymbol{k}$ space where the Fermi arc exists. As p decreases, the Fermi arc shrinks in the nodal (π, π) direction.[6,13] This model sufficiently explains the anomalous J_c suppression in underdoped Bi2212. According to the $\boldsymbol{k}$-space inhomogeneity model, the enlarged J_c/J_c^{AB} found in BiPb2212 implies a longer Fermi arc for BiPb2212 than that for Bi2212. Suzuki *et al.* found that the length of Fermi arc influences the observed tunneling spectra;[15] as Fermi arc increases, the heights of superconducting peaks increase and the dip-hump characteristic becomes less pronounced. Figure 6 shows the comparison between normalized tunneling spectra of a Bi2212 and a BiPb2212 sample with similar doping. The increase in the height of the superconducting peak and the repression of the dip-hump structure in BiPb2212 (indicated by red arrows) are consistent with the simulations of Suzuki *et al.* Therefore, we argue that the Pb substitution expands the length of the Fermi arc, which raises the J_c/J_c^{AB} in the underdoped region.

IV. CONCLUSIONS

We have analyzed the BiPb2212 system in the underdoped region by intrinsic tunneling spectroscopy. The Δ are identical to those of Bi2212, although the J_c's are significantly higher. The deviation of J_c from J_c^{AB} was found to be smaller than that for Bi2212. By comparing the tunneling spectra between BiPb2212 and Bi2212 with the numerical results,[15] we conclude that the observed J_c increase in Pb-substituted Bi cuprates results from not merely the reduced tunnel barrier but also elongation of the Fermi arc in the $\boldsymbol{k}$ space.

ACKNOWLEDGMENTS

---

*kambara@sk.kuee.kyoto-u.ac.jp

†kakeya@kuee.kyoto-u.ac.jp

[1] R. Kleiner and P. Müller, Phys. Rev. B **49**, 1327 (1994).

[2] M. Suzuki, T. Watanabe, and A. Matsuda, Phys. Rev. Lett. **82**, 5361 (1999).

[3] M. Suzuki and T. Watanabe, Phys. Rev. Lett. **85**, 4787 (2000).

[4] V. M. Krasnov, A. E. Kovalev, A. Yurgens, and D. Winkler, Phys. Rev. Lett. **86**, 2657 (2001).

[5] M. R. Norman, H. Ding, M. Randeria, J. C. Campuzano, T. Yokoya, T. Takeuchi, T. Takahashi, T. Mochiku, K. Kadowaki, P. Guptasarma, and D. G. Hinks, Nature (London) **392**, 157 (1998).

[6] W. S. Lee, I. M. Vishik, K. Tanaka, D. H. Lu, T. Sasagawa, N. Nagaosa, T. P. Devereaux, Z. Hussain, and Z.-X. Shen, Nature (London) **450**, 81 (2007).

[7] T. Kondo, R. Khasanov, T. Takeuchi, J. Schmalian, and A. Kaminski, Nature (London) **457**, 296 (2009).

[8] S. H. Pan, J. P. O'Neal, R. L. Badzey, C. Chamon, H. Ding, J. R. Engelbrecht, Z. Wang, H. Eisaki, S. Uchida, A. K. Gupta, K.-W. Ng, E. W. Hudson, K. M. Lang, and J. C. Davis, Nature (London) **413**, 282 (2001).

[9] G. Kinoda, T. Hasegawa, S. Nakao, T. Hanaguri, K. Kitazawa, K. Shimizu, J. Shimoyama, and K. Kishio, Phys. Rev. B **67**, 224509 (2003).

[10] A. Sugimoto, S. Kashiwaya, H. Eisaki, H. Kashiwaya, H. Tsuchiura, Y. Tanaka, K. Fujita, and S. Uchida, Phys. Rev. B **74**, 094503 (2006).

[11] T. Timusk and B. Statt, Rep. Prog. Phys. **62**, 61 (1999).

[12] A. Kanigel, M. R. Norman, M. Randeria, U. Chatterjee, S. Souma, A. Kaminski, H. M. Fretwell, S. Rosenkranz, M. Shi, T. Sato, T. Takahashi, Z. Z. Li, H. Raffy, K. Kadowaki, D. Hinks, L. Ozyuzer, and J. C. Campuzano, Nat. Phys. **2**, 447 (2006).

[13] T. Yoshida, X. J. Zhou, K. Tanaka, W. L. Yang, Z. Hussain, Z.-X. Shen, A. Fujimori, S. Sahrakorpi, M. Lindroos, R. S. Markiewicz, A. Bansil, S. Komiya, Y. Ando, H. Eisaki, T. Kakeshita, and S. Uchida, Phys. Rev. B **74**, 224510 (2006).

[14] V. Ambegaokar and A. Baratoff, Phys. Rev. Lett. **10**, 486 (1963).

[15] M. Suzuki, T. Hamatani, K. Anagawa, and T. Watanabe, Phys. Rev. B **85**, 214529 (2012).

[16] I. Chong, Z. Hiroi, M. Izumi, J. Shimoyama, Y. Nakayama, K. Kishio, T. Terashima, Y. Bando, and M. Takano, Science **276**, 770 (1997).

[17] T. Motohashi, Y. Nakayama, T. Fujita, K. Kitazawa, J. Shimoyama, and K. Kishio, Phys. Rev. B **59**, 14080 (1999).

[18] R. Gladyshevskii, N. Musolino, and R. Flükiger, Phys. Rev. B **70**, 184522 (2004).

[19] H. Kambara, I. Kakeya, and M. Suzuki, Physica C **471**, 754 (2011).

[20] I. Kakeya, K. Hamada, T. Tachiki, T. Watanabe, and M. Suzuki, Supercond. Sci. Technol. **22**, 114014 (2009).

[21] S. P. Zhao, X. B. Zhu, Y. F. Wei, G. H. Chen, Q. S. Yang, and C. T. Lin, Phys. Rev. B **72**, 184511 (2005).

[22] N. E. Hussey, J. Phys.: Condens. Matter **20**, 123201 (2008).

[23] W. Que and M. B. Walker, Phys. Rev. B **46**, 14772 (1992).

[24] D. Grebille, H. Leligny, A. Ruyter, P. Labbé, and B. Raveau, Acta Crystallogr. Sect. B **52**, 628 (1996).

[25] Y. Ando, Y. Hanaki, S. Ono, T. Murayama, K. Segawa, N. Miyamoto, and S. Komiya, Phys. Rev. B **61**, R14956 (2000).

[26] Z. Konstantinović, Z. Z. Li, and H. Raffy, Phys. Rev. B **62**, R11989 (2000).

[27] J. L. Tallon, C. Bernhard, H. Shaked, R. L. Hitterman, and J. D. Jorgensen, Phys. Rev. B **51**, 12911 (1995).

[28] Y. He, T. S. Nunner, P. J. Hirschfeld, and H.-P. Cheng, Phys. Rev. Lett. **96**, 197002 (2006).

[29] Y. He, S. Graser, P. J. Hirschfeld, and H.-P. Cheng, Phys. Rev. B **77**, 220507R (2008).

[30] A. Sugimoto, S. Kashiwaya, H. Eisaki, H. Yamaguchi, K. Oka, H. Kashiwaya, H. Tsuchiura, and Y. Tanaka, Physica C **426-431**, 390 (2005).

[31] Y. Kotaka, T. Kimura, H. Ikata, J. Shimoyama, K. Kitazawa, K. Yamafuji, K. Kishio, and D. Pooke, Physica C **235-240**, 1529 (1994).

[32] H. B. Wang, S. Guénon, B. Gross, J. Yuan, Z. G. Jiang, Y. Y. Zhong, M. Grünzweig, A. Iishi, P. H. Wu, T. Hatano, D. Koelle, and R. Kleiner, Phys. Rev. Lett. **105**, 057002 (2010).

[33] Y. Tanaka and S. Kashiwaya, Phys. Rev. B **56**, 892 (1997).

[34] M. Suzuki, T. Hamatani, Y. Yamada, K. Anagawa, and T. Watanabe, J. Phys.: Conf. Ser. **43**, 1110 (2006).